

Inelastic squared form factors of the vibronic states of $B^1\Sigma_u^+$, $C^1\Pi_u$, and $EF^1\Sigma_g^+$ for molecular D_2 studied by high-energy electron scattering

Ya-Wei Liu,^{1,2,3} Shu-Xing Wang^{1,*}, Long-Quan Xu,¹ Yi-Geng Peng,⁴ Song-Bin Zhang⁵, Yong Wu,^{4,6,†}
Jian-Guo Wang,⁴ and Lin-Fan Zhu^{1,‡}

¹Hefei National Research Center for Physical Sciences at Microscale and Department of Modern Physics, University of Science and Technology of China, Hefei, Anhui 230026, People's Republic of China

²Anhui Province Key Laboratory of Medical Physics and Technology, Institute of Health and Medical Technology, Hefei Institutes of Physical Science, Chinese Academy of Sciences, Hefei, Anhui 230031, People's Republic of China

³State Key Laboratory of Molecular Reaction Dynamics, Dalian Institute of Chemical Physics, Chinese Academy of Sciences, Dalian, Liaoning 116023, People's Republic of China

⁴Institute of Applied Physics and Computational Mathematics, Beijing 100088, People's Republic of China

⁵School of Physics and Information Technology, Shaanxi Normal University, Xi'an, Shaanxi 710119, People's Republic of China

⁶HEDPS, Center for Applied Physics and Technology, Peking University, Beijing 100084, People's Republic of China



(Received 31 October 2022; accepted 26 January 2023; published 6 February 2023)

The inelastic squared form factors of the valence-shell excitations of D_2 were measured by high-energy electron scattering and calculated by the multireference single- and double-excitation configuration interaction method in the present work. It is found that for the $B^1\Sigma_u^+$ state of D_2 , the theoretical calculation cannot satisfactorily reproduce the inelastic squared form factors with a higher vibrational quantum number. For the vibronic states of $C^1\Pi_u$ and $EF^1\Sigma_g^+$ of D_2 , obvious discrepancies between our electron-scattering results and theoretical calculations are found. Similar phenomena observed for H_2 , HD, and D_2 may be attributed to electronic-vibrational coupling and the failure of the first Born approximation at an incident electron energy of 1500 eV. Furthermore, the present inelastic squared form factors of D_2 are in good agreement with the ones of H_2 and HD, which indicates that there is no isotope effect for the electronic matrix elements of H_2 , HD, and D_2 in the momentum space.

DOI: [10.1103/PhysRevA.107.022803](https://doi.org/10.1103/PhysRevA.107.022803)

I. INTRODUCTION

Molecular hydrogen (H_2) and its isotopomers, i.e., molecular hydrogen deuteride (HD) and deuterium (D_2), play important roles in planetary atmospheres [1], star formation [2], and tokamak edge plasmas [3–6]. The electron-scattering cross sections of H_2 and its isotopomers are the basic input parameters of theoretical models to simulate physical and chemical processes in the environments mentioned above. The demand for these data has increased in recent years. For example, as abundant components in the edge region of fusion devices, HD and D_2 molecules are produced near plasma-facing components such as limiters or divertors in tokamak edge plasmas [3–6]. The cross-section data of HD and D_2 are crucial in understanding the boundary condition and the plasma-wall interaction in fusion plasmas. However, the data available nowadays cannot meet the demands in the variety of areas mentioned above. As pointed out in the recent review by Yoon *et al.* [7], the paucity of HD and D_2 data by electron scattering leaves us with a partially incomplete picture of the electron-impact cross sections of H_2 and its isotopomers. Furthermore, H_2 , HD, and D_2 molecules are

the simplest molecular two-electron systems and are therefore of interest for quantum mechanical calculations beyond the Born-Oppenheimer approximation [8]. Recently, we measured the inelastic squared form factors [9,10] and the optical oscillator strengths [11,12] of H_2 and its isotopomers by high-energy electron scattering and high-resolution inelastic x-ray scattering methods. As one of a series of works for the accurate measurement of the dynamic parameters of H_2 and its isotopomers HD and D_2 , the main purpose of the present work is to supplement the dynamic parameters of molecular D_2 by high-energy electron scattering.

Dynamic parameters such as the inelastic squared form factors, generalized oscillator strengths, as well as differential and integral cross sections of H_2 and its isotopomers HD and D_2 are valuable due to their extensive applications. However, experimental measurements are still scarce, except for H_2 . The main experimental difficulties are to resolve the heavily overlapped bands and to determine the absolute values. The experimental investigations of the dynamic parameters of H_2 and HD have been summarized in our recent works [9,10]. For the D_2 molecule, its electron-energy loss spectrum in the region of the Lyman and Werner bands was measured by Geiger and Schmoranzler [13] at an incident electron energy of 34 keV and an energy resolution of about 10 meV with near zero momentum transfer. The intensity distributions of the Lyman and Werner bands were obtained, in which a considerable isotope effect, i.e., the maximum intensity shift

* wangshuxing@ustc.edu.cn

† wuyong@iapcm.ac.cn

‡ lfzhu@ustc.edu.cn

and vibrational level interval variation, was observed. After that, Becker and McConkey [14] studied the Lyman and Werner band emissions of D₂ produced at incident electron energies of 20–500 eV, and Abgrall *et al.* [15] measured the high-resolution emission spectra of D₂ excited by an electron beam with an energy of 100 eV.

Similarly, the previous theoretical calculations for the dynamic parameters of H₂ and HD were also summarized in our recent papers [9,10]. For the D₂ molecule, the only calculation is about the generalized oscillator strengths of the vibronic states of the Lyman band by Kolos *et al.* [16] with the wave functions expanded in an explicitly correlated Gaussian function. In addition, Fantz and Wunderlich [8] have reported the Franck-Condon factors, transition probabilities, and radiative lifetimes for H₂, HD, and D₂, on the basis of the latest Born-Oppenheimer potential curves and the latest electronic dipole transition moments of H₂.

According to Bethe theory [17–20], the inelastic squared form factor can be determined from the experimental differential cross section or generalized oscillator strength measured by the high-energy electron-energy loss spectroscopy [21–23] within the first Born approximation,

$$\begin{aligned} \zeta(\mathbf{q}, \omega_n) &= \left| \langle \Psi_n | \sum_{j=1}^N \exp(i\mathbf{q} \cdot \mathbf{r}_j) | \Psi_0 \rangle \right|^2 = \frac{1}{4} \frac{k_i}{k_f} q^4 \left(\frac{d\sigma}{d\Omega} \right)_e \\ &= \frac{q^2}{2\omega_n} f(\mathbf{q}, \omega_n). \end{aligned} \quad (1)$$

Here, Ψ_0 and Ψ_n are the N -electron wave functions for the initial and final states, while ω_n and \mathbf{q} are the excitation energy and momentum transfer, respectively. The sum is over all electrons, and \mathbf{r}_j is the position vector of the j th electron. k_i and k_f are the magnitudes of the momenta of the incident and scattered electrons, respectively. $(\frac{d\sigma}{d\Omega})_e$ and $f(\mathbf{q}, \omega_n)$ are the differential cross section and generalized oscillator strength measured by the high-energy electron-energy loss spectroscopy. It should be noted that the inelastic squared form factors, generalized oscillator strengths, and differential cross sections are all fundamental physical quantities commonly used, and they can be mutually converted according to Eq. (1).

In this work, the inelastic squared form factors for the vibronic excitations of the Lyman band, the Werner band, and the $EF^1\Sigma_g^+$ state of the D₂ molecule were measured by the high-energy electron-energy loss spectroscopy and calculated by the multireference single- and double-excitation configuration interaction method. This paper is organized as follows. The experimental procedure and calculational method are described in Sec. II. The inelastic squared form factors of the valence-shell excitations of D₂ are then compared and discussed in detail in Sec. III. The summary and conclusions are presented in Sec. IV.

II. EXPERIMENTAL PROCEDURE AND CALCULATIONAL METHOD

The present electron-energy loss spectroscopy experiment was carried out with a high-resolution fast electron-energy

loss spectrometer, which has been described in detail in the previous works [24,25]. In this experiment, the incident electron energy was set at 1500 eV and the energy resolution was about 70 meV. The electron-energy loss spectra of D₂ at different scattering angles from 1.5° to 8° were recorded at room temperature. To simplify the normalization procedure and improve the accuracy of the experimental results, the standard relative flow technique [26–28] was used in the present experiment. In brief, the flow rates of helium and D₂ were controlled, respectively, by two flow meters with an accuracy of better than 2%. The gases were mixed together before flowing into the interaction chamber continuously through a jet nozzle. Then, the intensity ratios of the valence-shell excitations of D₂ to the 2^1P state of helium were determined according to the measured energy loss spectra, and therefore the inelastic squared form factors of D₂ were determined by referencing to the data of helium, which has been measured and calculated with a high accuracy [24,29–31]. The normalization procedures were described in detail in our recent papers [27,28,32]. A typical electron-energy loss spectrum of the valence-shell excitations of D₂ is shown in Fig. 1(a) along with the excited states assigned according to the theoretical calculations of Fantz and Wunderlich [8]. By calibrating the electron-energy loss spectrum at each scattering angle into the absolute scale, the two-dimensional inelastic squared form factor densities (ISFFDs) of the valence-shell excitations of D₂ versus the energy loss and the squared momentum transfer were obtained and are shown in Fig. 1(b).

From the electron-energy loss spectra measured at different scattering angles, the intensities of the vibronic excitations of D₂ were obtained by a modified least-squares fitting method [33], which has been used in our recent works [9–12]. The key to this method is that the intensity distribution of the vibronic transitions of the $B^1\Sigma_u^+$ or $C^1\Pi_u$ electronic state of the D₂ molecule is delineated by the calculated ones modified by a linear scaling function varying with the energy level of the vibronic state, which accounts for the deviation from the Franck-Condon principle. Meanwhile, the intensity of every vibronic transition of the $EF^1\Sigma_g^+$ electronic state is fitted by an independent peak in view of its possible anomalous vibronic intensity distribution at different momentum transfers due to the two minima of its potential curve resulting from the avoided crossing. Similar anomalous phenomena have also been observed and investigated for the $B^1\Sigma^+$ state of CO [34,35] and $E^3\Sigma_u^-$ state of O₂ [35–38]. Considering the thermal distribution of the initial rotational levels and the different intervals of the final rotational levels for the different electronic states, a Gaussian function with the same full width at half maximum was used to describe the vibronic transitions in an electronic state, while different full width at half maximums were used for different electronic states.

The experimental errors of the present inelastic squared form factors of D₂ include the contributions from the definite angular resolution, the angle determination, the statistical counts, the fitting procedure, and the normalizing procedure. The total experimental errors are approximately 5–10% for most of the resolved vibronic states, and up to 10–30% for some unresolved vibronic states, which are shown in the corresponding figures. The inelastic squared form factors, generalized oscillator strengths, and differential cross

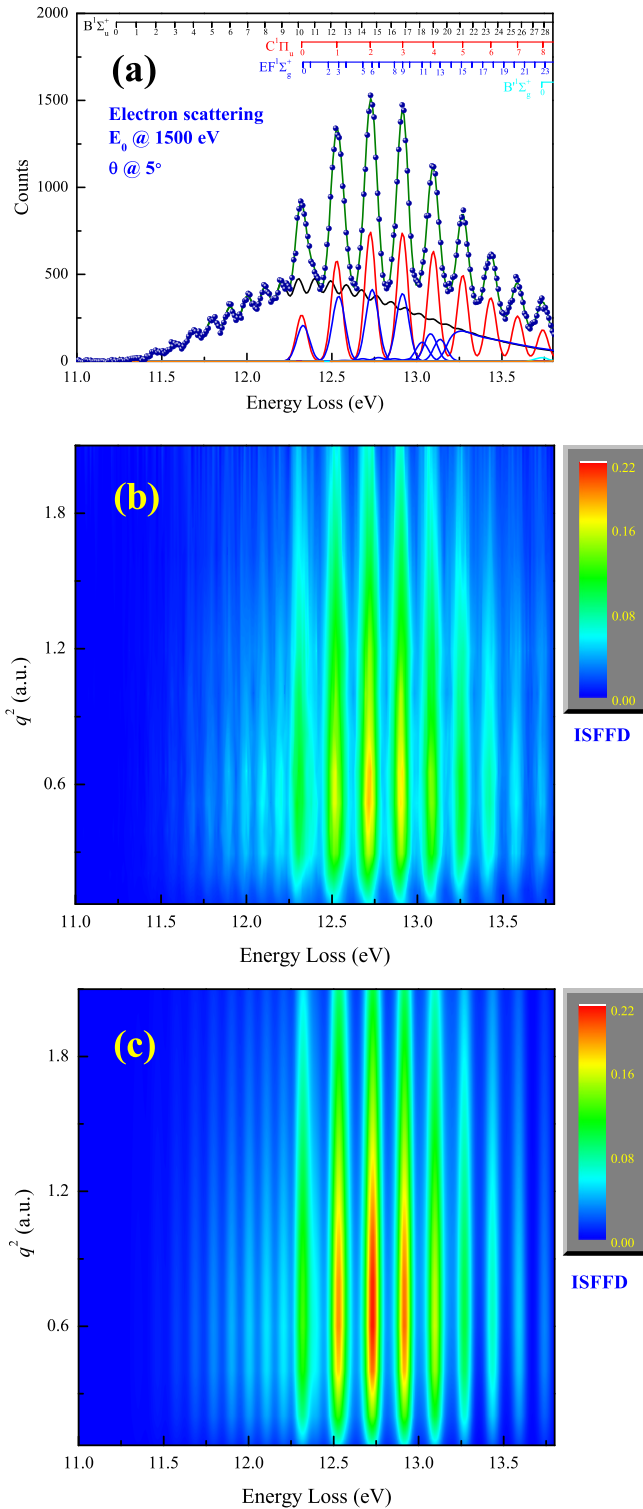


FIG. 1. (a) A typical electron-energy loss spectrum of the valence-shell excitations of D_2 at an incident electron energy of 1500 eV and a scattering angle of 5° . Solid lines are the fitted curves. (b),(c) Present measured and calculated two-dimensional maps for the inelastic squared form factor densities of D_2 vs the energy loss and squared momentum transfer.

sections of the vibronic states of the $B^1\Sigma_u^+$, $C^1\Pi_u$, and $EF^1\Sigma_g^+$ electronic states of D_2 are tabulated in the Supplemental Material [39].

We also calculated the inelastic squared form factors of the vibronic states of the $B^1\Sigma_u^+$, $C^1\Pi_u$, and $EF^1\Sigma_g^+$ electronic states of D_2 with the multireference single- and double-excitation configuration interaction method [40–42], and this method has been used to calculate the inelastic squared form factors and generalized oscillator strengths of the valence-shell excitations of H_2 [9], HD [10], H_2O [43,44], and N_2 [45] in our recent works. The multireference single- and double-excitation configuration interaction method can balance the computational complexity and accuracy for the calculation of the ground state and excited state of a multielectron system. For the two-electron system of the D_2 molecule, the full configuration interaction method not only achieves a high precision, but also costs a small amount of calculation. Under this circumstance, the nonrelativistic self-consistent field calculations were performed in the D_{2h} symmetry group, and the resulting molecular orbitals were used to construct the Hartree-Fock and configuration interaction wave functions of the D_2 molecule. With the Gaussian basis set of (6s, 5p, 4d, 1f) applied, approximately 1200 configurations were included in the full-configuration-interaction calculations for different internuclear distances. It should be noted that in addition to the quadruple- ζ Gaussian basis sets, the correlation-consistent polarized valence double zeta and triple zeta (i.e., cc-PVDZ, cc-PVTZ) ones have also been applied to perform the calculations to ensure the convergence of the present calculation.

The Born-Oppenheimer potential-energy curves and the absolute asymptotic energies (i.e., the energies at very large internuclear distances) for the $B^1\Sigma_u^+$, $C^1\Pi_u$, and $EF^1\Sigma_g^+$ electronic states of D_2 were calculated in the present work. Using the adiabatic potential-energy curves obtained above, the nuclear vibronic energies and wave functions can be obtained by solving the one-dimensional radial Schrodinger equation, where the discrete variable representation method [46] has been used. Note that the computational precision is higher than 10^{-8} a.u. in the present calculation. Based on the calculated electronic and vibronic wave functions, the electronic-vibronic inelastic squared form factors can be obtained. For freely rotating molecules, it should compare an orientation-averaged result with the experimental data, which has been done by holding the molecule fixed and allowing the momentum transfer \mathbf{q} to change its relative orientation.

The calculated two-dimensional inelastic squared form factor density map of D_2 versus the energy loss and the squared momentum transfer is shown in Fig. 1(c), with the theoretical inelastic squared form factors convoluted by the present experimental energy resolution of 70 meV.

III. RESULTS AND DISCUSSION

As shown in Figs. 1(b) and 1(c), the present electron-energy loss spectra and theoretical inelastic squared form factor densities qualitatively coincide with both their absolute scales and momentum transfer dependence behaviors. Compared with its isotopomers H_2 [9] and HD [10], the D_2 molecule has denser vibronic excitations for every electronic state. Under this circumstance, the present experimental and theoretical inelastic squared form factors for some selected

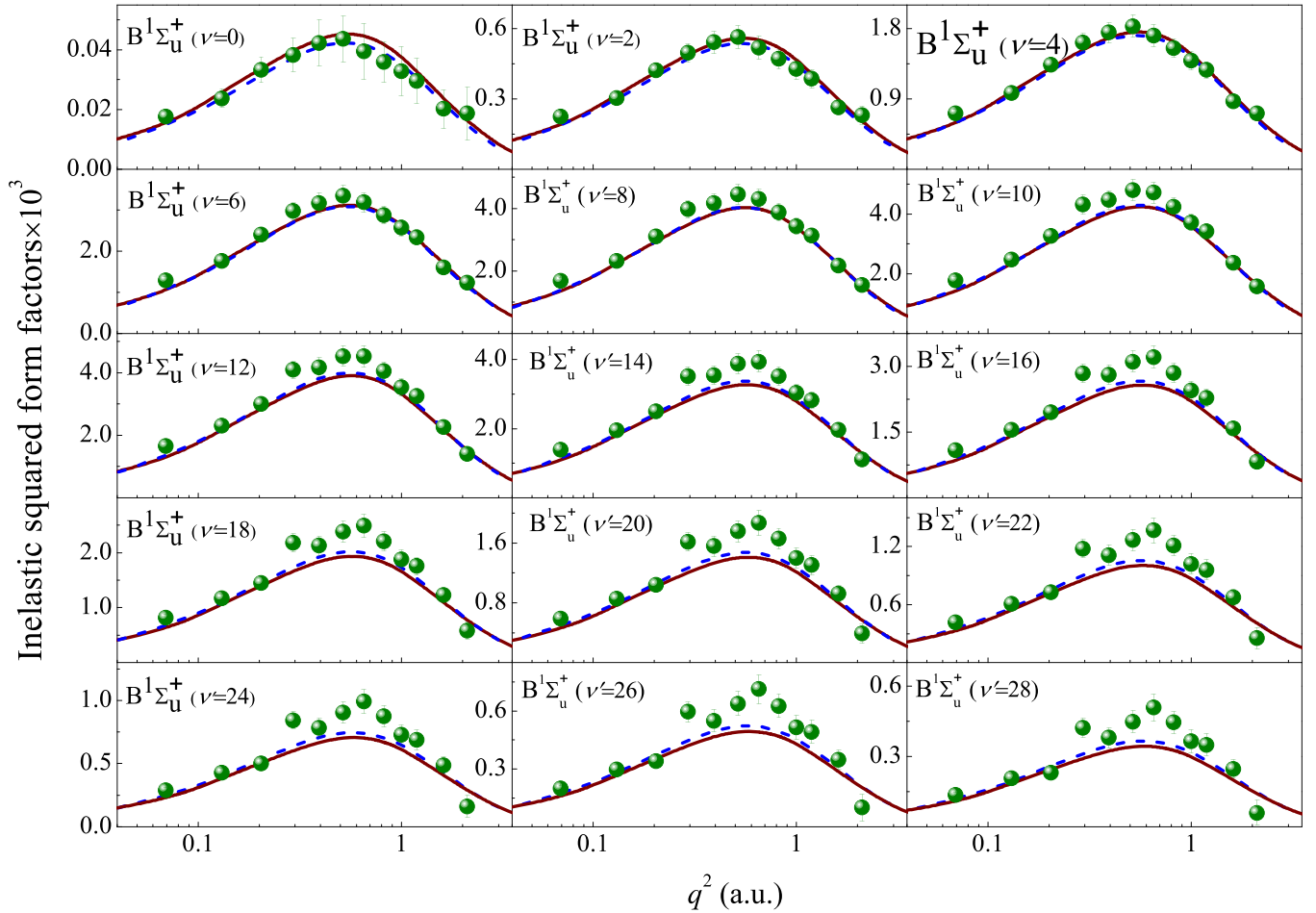


FIG. 2. The selected inelastic squared form factors of the Lyman band of the D_2 molecule. Green spheres: the present electron-energy loss spectroscopy results. Brown solid lines: the present calculations by the multireference single- and double-excitation configuration interaction method. Blue dash-dotted lines: the theoretical results of Kolos *et al.* [16].

vibronic states of the $B^1\Sigma_u^+$, $C^1\Pi_u$, and $EF^1\Sigma_g^+$ electronic states of the D_2 molecule are compared with the previously available results [16] in Figs. 2–4 for clarity.

Figure 2 shows that the present theoretical inelastic squared form factors of $B^1\Sigma_u^+(v' = 0 - 28)$ by the multireference single- and double-excitation configuration interaction method are in agreement with the ones by Kolos *et al.* [16], although the results of Kolos *et al.* [16] are slightly lower than the present calculations for the lower vibronic states, while the situation is reversed for higher vibronic states. As shown in Fig. 1(a), the vibronic states of $B^1\Sigma_u^+(v' \leq 9)$ do not overlap with other electronic states, so the present experimental inelastic squared form factors of $B^1\Sigma_u^+(v' \leq 9)$ are free from any systematic errors from the fitting procedure. The good agreement between the experimental and theoretical results indicates the reliability of the present results. However, gradual deviations of the experimental data from the theoretical calculations for the higher vibrational states are noticeable, and similar phenomena have also been observed for the Lyman bands of molecular H_2 [9] and HD [10]. The discrepancies between the electron-energy loss spectroscopy results and the calculated results for higher vibronic states

of $B^1\Sigma_u^+$ of H_2 [9], HD [10], and D_2 may be due to the electronic-vibronic coupling effect. Although the influence of the electronic-vibronic coupling effect on the emission probabilities and transition energies has been studied by Abgrall *et al.* [47] and Wolniewicz *et al.* [48], no scattering dynamic parameter such as the inelastic squared form factor or generalized oscillator strength with the electronic-vibronic coupling effect accounted has been reported.

The present experimental and theoretical inelastic squared form factors for the vibronic states of the Werner band are shown in Fig. 3. Unfortunately, there are no other theoretical and experimental results for comparison. Similar to molecular H_2 [9] and HD [10], random allocations of the intensities may exist for the vibronic states of $C^1\Pi_u$ and $EF^1\Sigma_g^+$ of molecular D_2 because of the near match of their energy positions, which may introduce somewhat larger experimental errors into the fitting procedure. It is clear in Fig. 3 that the present experimental inelastic squared form factors of the vibronic states of the Werner band are obviously lower than the present calculations by the multireference single- and double-excitation configuration interaction method, while the discrepancies decrease in the low- q^2 region. The same phe-

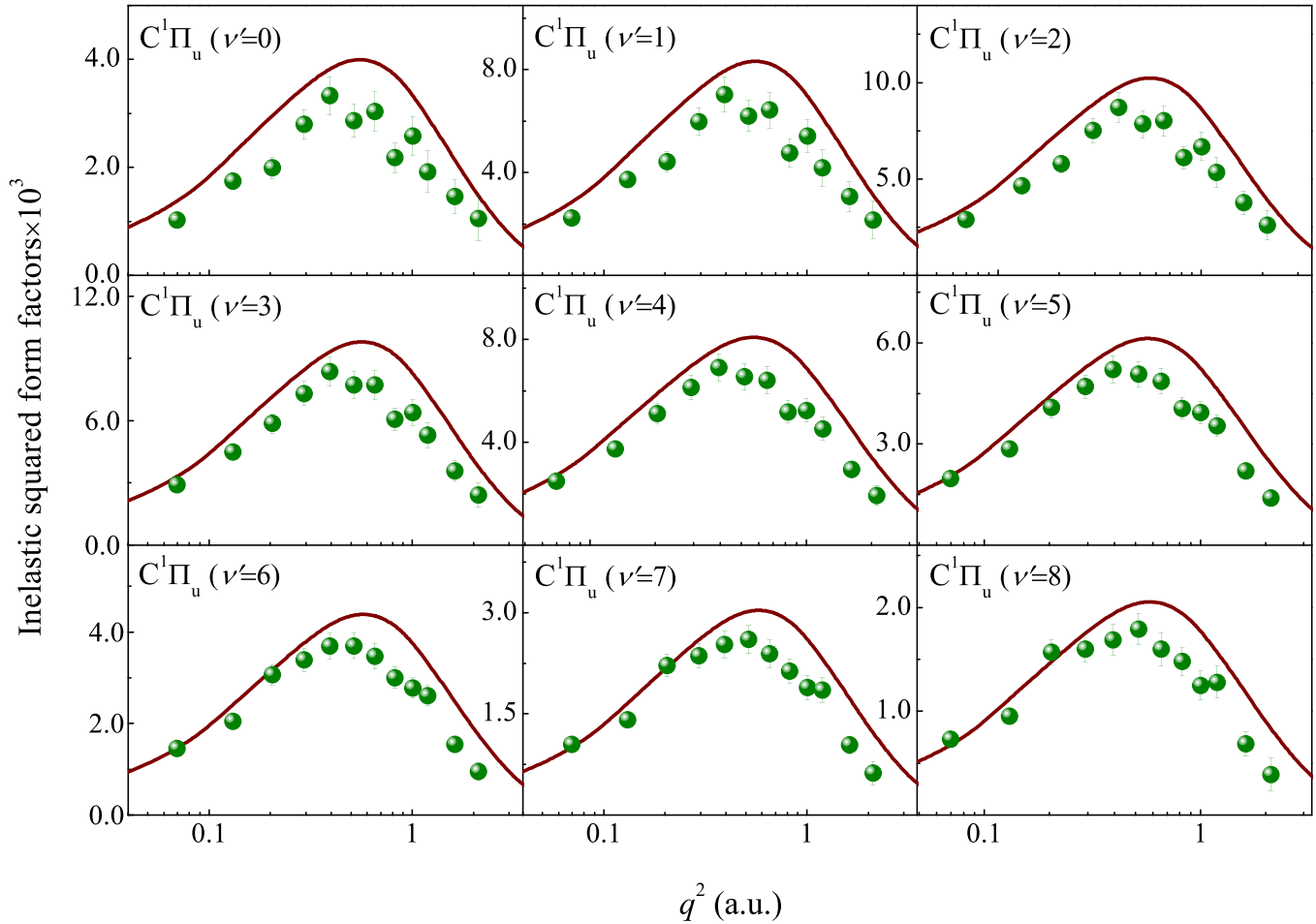


FIG. 3. The selected inelastic squared form factors of the Werner band of the D_2 molecule. Green spheres: the present electron-energy loss spectroscopy results; brown solid lines: the present calculations by the multireference single- and double-excitation configuration interaction method.

nomenon was also observed for the Werner band of molecular HD, while reasonable agreement between the experimental results and the calculations by the multireference single- and double-excitation configuration interaction method is achieved for H_2 [9]. To elucidate this phenomenon, more experimental and theoretical investigations are strongly recommended.

Figure 4(a) shows the present inelastic squared form factors of the vibronic states of the $EF^1\Sigma_g^+$ electronic state of the D_2 molecule. The irregular Franck-Condon factors of $EF^1\Sigma_g^+$ induced by the double-well potential curve [8] make fitting its vibronic intensities difficult, and the heavy overlap with the Werner band makes the situation more severe, so the inelastic squared form factors of the vibronic states of $EF^1\Sigma_g^+$ show apparent irregularities and fluctuations. Despite this, the present experimental inelastic squared form factors of $EF^1\Sigma_g^+$ are in reasonable agreement with the present calculations by the multireference single- and double-excitation configuration interaction method.

To avoid possible systematic errors from the fitting procedures for the heavily overlapped states in the energy region larger than 12.2 eV, the sum inelastic squared form factors

of the vibronic states of $C^1\Pi_u$ and $EF^1\Sigma_g^+$ are shown in Fig. 4(b). It is clear that the present experimental results are generally lower than the present calculations by the multireference single- and double-excitation configuration interaction method, especially in the large squared momentum transfer region. A similar phenomenon was also observed for the H_2 [9] and HD molecules [10]. However, the inelastic squared form factors of each vibronic state of $C^1\Pi_u$ (including contributions of the $EF^1\Sigma_g^+$ state) of H_2 by the inelastic x-ray scattering [9], which always follows the first Born approximation, are in good agreement with the theoretical ones [9,16]. Therefore, it is likely that the first Born approximation is not valid in the larger squared momentum transfer region at the incident electron energy of 1500 eV for H_2 [9] and its isotopomers HD [10] and D_2 .

It is always an interesting topic whether there is an isotope effect in the electronic transitions for molecules [7,49,50]. Although the vibronic-rotational transition energies and their Franck-Condon factors are clearly influenced by the isotope effect [13], it is generally believed that the electronic transition matrix element is free from the isotopic atomic substitution in a molecule [49]; however, there is a lack of

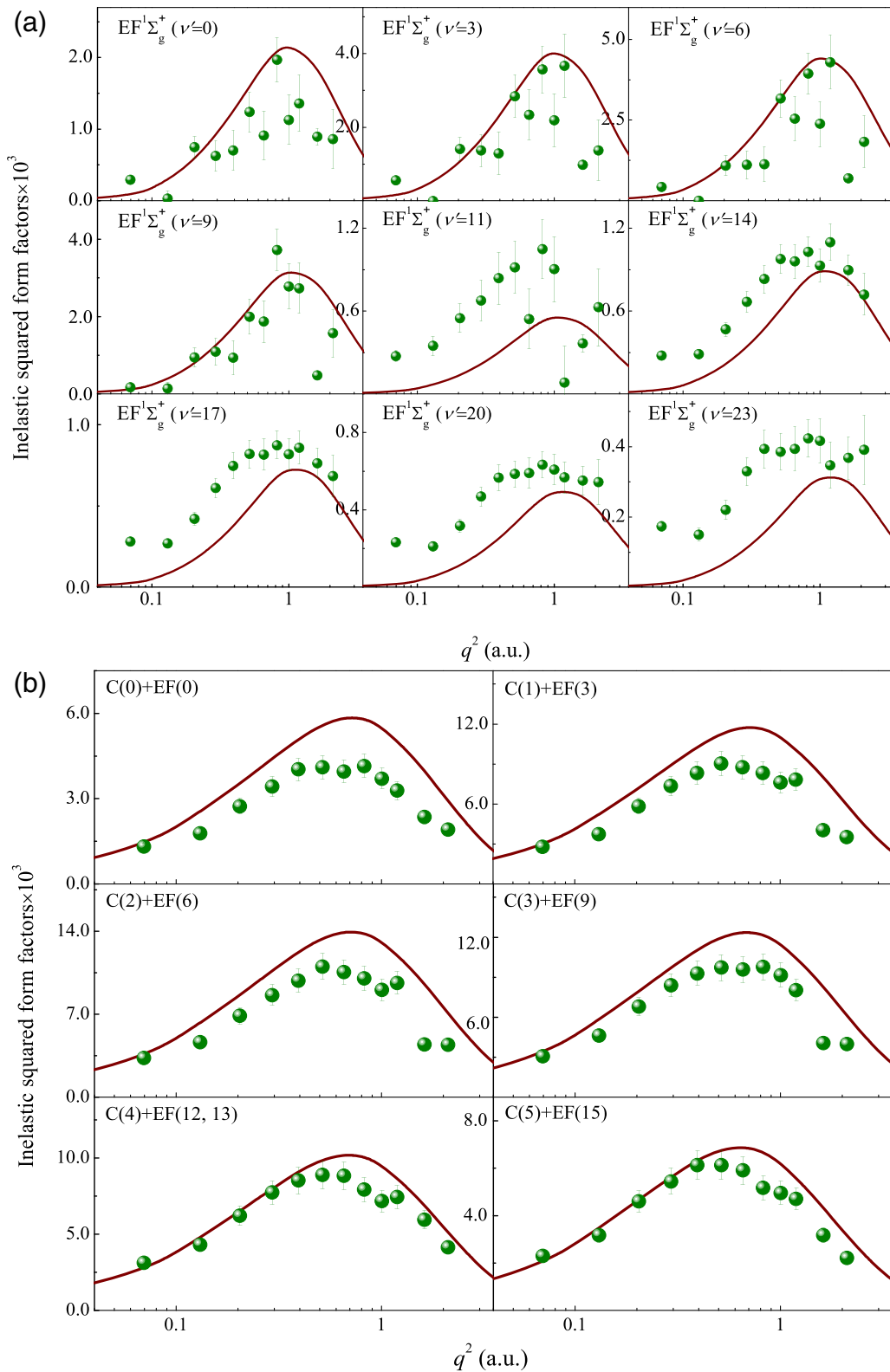


FIG. 4. (a) The selected inelastic squared form factors of the $EF^1\Sigma_g^+$ electronic state of the D_2 molecule. (b) The selected sum inelastic squared form factors of the vibronic states belonging to the Werner band and the $EF^1\Sigma_g^+$ electronic state of the D_2 molecule. Green spheres: the present electron-energy loss spectroscopy results; brown solid lines: the present calculations by the multireference single- and double-excitation configuration interaction method.

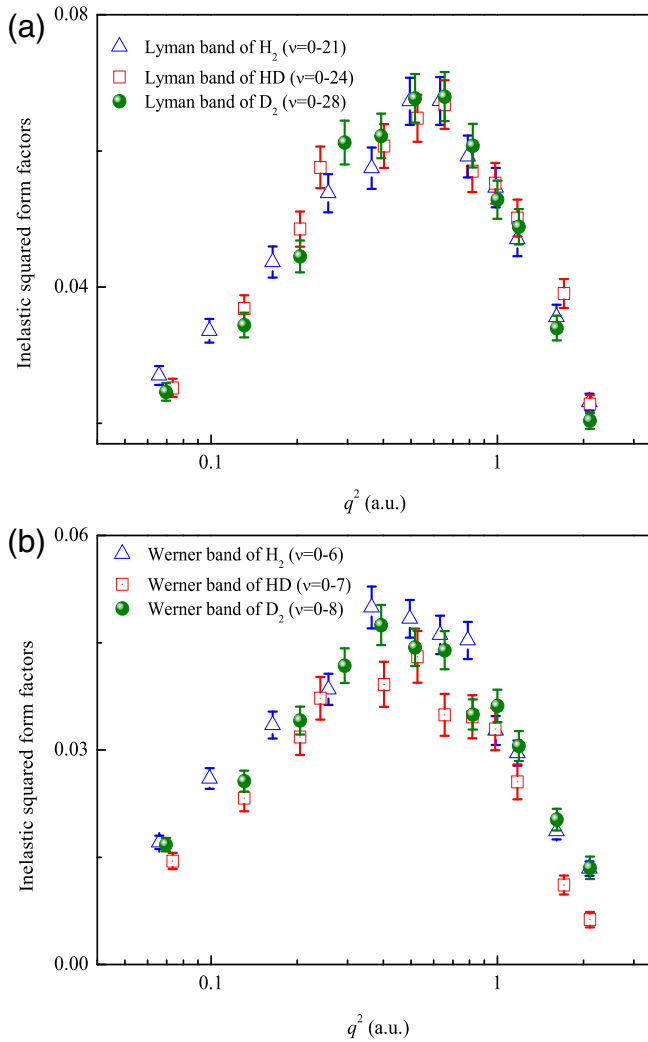


FIG. 5. (a) The sum inelastic squared form factors of the Lyman band of $H_2(v=0-21)$ [9], $HD(v=0-24)$ [10], and $D_2(v=0-28)$. (b) The sum inelastic squared form factors of the Werner band of $H_2(v=0-6)$ [9], $HD(v=0-7)$ [10], and $D_2(v=0-8)$.

experimental evidence. Figure 5 shows the inelastic squared form factors for the Lyman and Werner bands from light H_2 to heavy HD and D_2 in the whole squared momentum transfer region [9,10]. It is clear that the experimental data for different isotopomers are in agreement within experimental uncertainties, so Fig. 5 indicates that the isotope effect has no apparent influence on the electronic transition procedure of

H_2 and its isotopomers HD and D_2 , which follows the general understanding of the isotope effect.

IV. SUMMARY AND CONCLUSION

The present work is the last one of this series of works for the measurement of the dynamic parameters of H_2 and its isotopomers HD and D_2 [9,10]. In this series of works, joint experimental and theoretical investigations of the inelastic squared form factors of the vibronic states of the $B^1\Sigma_u^+$, $C^1\Pi_u$, and $EF^1\Sigma_g^+$ electronic states of molecular H_2 , HD , and D_2 have been performed. It is found that the discrepancies in the inelastic squared form factors of $B^1\Sigma_u^+$ between our electron-energy loss spectroscopy results and the theoretical calculations become larger with increasing vibrational quantum numbers, and this phenomenon gradually weakens with increasing molecular weight from molecular H_2 [9], HD [10], to D_2 , which may be due to the electronic-vibronic coupling effect. Furthermore, the inelastic squared form factors of the vibronic states of $C^1\Pi_u$ (including contributions of the $EF^1\Sigma_g^+$ state) of H_2 [9], HD [10], and D_2 by the electron-energy loss spectroscopy are slightly lower than the present calculations by the multireference single- and double-excitation configuration interaction method and the inelastic x-ray scattering ones of H_2 , which indicates that the first Born approximation may be invalid in the larger squared momentum transfer region at the incident electron energy of 1500 eV. The quantitative comparisons for the inelastic squared form factors of H_2 , HD , and D_2 indicate that there is no apparent isotope effect for the electron-impact excitation, which follows the general understanding of the isotope effect. The present systematic works on the measurement of the dynamic parameters of H_2 and its isotopomers HD and D_2 will fill the gap of the data for both HD and D_2 to a large extent. Moreover, these dynamic parameters can be used as the basic input data for the study of planetary atmospheres, star formation, and tokamak edge plasmas.

ACKNOWLEDGMENTS

This work is supported by the National Natural Science Foundation of China (Grants No. 22073100 and No. U1932207), the Strategic Priority Research Program of the Chinese Academy of Sciences (Grant No. XDB34000000), and the Liaoning Natural Science Foundation (Grant No. 2020-MS-015).

[1] E. Lellouch, B. Bézard, T. Fouchet, H. Feuchtgruber, T. Encrenaz, and T. de Graauw, *Astron. Astrophys.* **370**, 610 (2001).
 [2] T. I. Ivanov, M. Roudjane, M. O. Vieitez, C. A. de Lange, W.-Ü L. Tchchang-Brillet, and W. Ubachs, *Phys. Rev. Lett.* **100**, 093007 (2008).
 [3] S. Brezinsek, P. T. Greenland, P. Mertens, A. Pospieszczyk, U. Samm, B. Schweer, and G. Sergienko, *Phys. Scr.* **T103**, 63 (2003).

[4] A. Pospieszczyk, S. Brezinsek, A. Meigs, P. Mertens, G. Sergienko, M. Stamp, and JET-EFDA Contributors, *J. Nucl. Mater.* **363-365**, 811 (2007).
 [5] A. Pospieszczyk, S. Brezinsek, G. Sergienko, P. T. Greenland, A. Huber, A. Meigs, P. Mertens, U. Samm, M. Stamp, and S. Wiesen, *J. Nucl. Mater.* **337-339**, 500 (2005).
 [6] E. M. Hollmann, S. Brezinsek, N. H. Brooks, M. Groth, A. G. McLean, A. Y. Pigarov, and D. L. Rudakov, *Plasma. Phys. Control. Fusion* **48**, 1165 (2006).

- [7] J. S. Yoon, Y. W. Kim, D. C. Kwon, M. Y. Song, W. S. Chang, C. G. Kim, V. Kumar, and B. J. Lee, *Rep. Prog. Phys.* **73**, 116401 (2010).
- [8] U. Fantz and D. Wünderlich, *At. Data Nucl. Data Tables* **92**, 853 (2006).
- [9] L. Q. Xu, X. Kang, Y. G. Peng, X. Xu, Y. W. Liu, Y. Wu, K. Yang, N. Hiraoka, K. D. Tsuei, J. G. Wang, and L. F. Zhu, *Phys. Rev. A* **97**, 032503 (2018).
- [10] L. Q. Xu, Y. G. Peng, T. Xiong, X. Xu, Y. W. Liu, Y. Wu, J. G. Wang, and L. F. Zhu, *Phys. Rev. A* **98**, 012502 (2018).
- [11] T. Xiong, Y. C. Xu, K. Yang, N. Hiraoka, and L. F. Zhu, *Astrophys. J.* **885**, 163 (2019).
- [12] T. Xiong, Y. W. Liu, K. Yang, X. C. Huang, S. X. Wang, S. Yan, K. L. Yu, N. Hiraoka, K. D. Tsuei, and L. F. Zhu, *Phys. Rev. A* **98**, 042509 (2018).
- [13] J. Geiger and H. Schmoranzler, *J. Mol. Spectrosc.* **32**, 39 (1969).
- [14] K. Becker and J. W. McConkey, *Can. J. Phys.* **62**, 1 (1984).
- [15] H. Abgrall, E. Roueff, X. Liu, D. E. Shemansky, and G. K. James, *J. Phys. B: At. Mol. Opt. Phys.* **32**, 3813 (1999).
- [16] W. Kolos, H. J. Monkhorst, and K. Szalewicz, *At. Data Nucl. Data Tables* **28**, 239 (1983).
- [17] H. Bethe, *Ann. Phys.* **397**, 325 (1930).
- [18] M. Inokuti, *Rev. Mod. Phys.* **43**, 297 (1971).
- [19] T. Northey, A. M. Carrascosa, S. Schäfer, and A. Kirrander, *J. Chem. Phys.* **145**, 154304 (2016).
- [20] A. M. Carrascosa, T. Northey, and A. Kirrander, *Phys. Chem. Chem. Phys.* **19**, 7853 (2017).
- [21] P. M. Platzman and N. Tzoar, *Phys. Rev.* **139**, A410 (1965).
- [22] P. Eisenberger and P. M. Platzman, *Phys. Rev. A* **2**, 415 (1970).
- [23] L. F. Zhu, L. S. Wang, B. P. Xie, K. Yang, N. Hiraoka, Y. Q. Cai, and D. L. Feng, *J. Phys. B: At. Mol. Opt. Phys.* **44**, 025203 (2011).
- [24] K. Z. Xu, R. F. Feng, S. L. Wu, Q. Ji, X. J. Zhang, Z. P. Zhong, and Y. Zheng, *Phys. Rev. A* **53**, 3081 (1996).
- [25] X. J. Liu, L. F. Zhu, X. M. Jiang, Z. S. Yuan, B. Cai, X. J. Chen, and K. Z. Xu, *Rev. Sci. Instrum.* **72**, 3357 (2001).
- [26] M. A. Khakoo and S. Trajmar, *Phys. Rev. A* **34**, 138 (1986).
- [27] Y. W. Liu, L. Q. Xu, D. D. Ni, X. Xu, X. C. Huang, and L. F. Zhu, *J. Geophys. Res.: Space Phys.* **122**, 3459 (2017).
- [28] Y. W. Liu, L. Q. Xu, T. Xiong, X. Chen, K. Yang, N. Hiraoka, K. D. Tsuei, and L. F. Zhu, *Astrophys. J. Suppl. Ser.* **238**, 26 (2018).
- [29] B. P. Xie, L. F. Zhu, K. Yang, B. Zhou, N. Hiraoka, Y. Q. Cai, Y. Yao, C. Q. Wu, E. L. Wang, and D. L. Feng, *Phys. Rev. A* **82**, 032501 (2010).
- [30] N. M. Cann and A. J. Thakkar, *J. Electron. Spectrosc. Relat. Phenom.* **123**, 143 (2002).
- [31] X. Y. Han and J. M. Li, *Phys. Rev. A* **74**, 062711 (2006).
- [32] D. D. Ni, L. Q. Xu, Y. W. Liu, K. Yang, N. Hiraoka, K. D. Tsuei, and L. F. Zhu, *Phys. Rev. A* **96**, 012518 (2017).
- [33] W. Q. Xu, Y. W. Liu, T. Xiong, X. C. Huang, S. X. Wang, X. X. Mei, X. Sun, X. Shi, and L. F. Zhu, *J. Electron. Spectrosc. Relat. Phenom.* **234**, 13 (2019).
- [34] Z. P. Zhong, R. F. Feng, K. Z. Xu, S. L. Wu, L. F. Zhu, X. J. Zhang, Q. Ji, and Q. C. Shi, *Phys. Rev. A* **55**, 1799 (1997).
- [35] M. Dillon, M. Kimura, R. J. Buenker, G. Hirsch, Y. Li, and L. Chantranupong, *J. Chem. Phys.* **102**, 1561 (1995).
- [36] Y. Li, M. Honigmann, K. Bhanuprakash, G. Hirsch, R. J. Buenker, M. A. Dillon, and M. Kimura, *J. Chem. Phys.* **96**, 8314 (1992).
- [37] M. Kimura, M. A. Dillon, R. J. Buenker, G. Hirsch, Y. Li, and L. Chantranupong, *Z. Phys. D* **38**, 165 (1996).
- [38] B. R. Lewis, J. P. England, S. T. Gibson, M. J. Brunger, and M. Allan, *Phys. Rev. A* **63**, 022707 (2001).
- [39] See Supplemental Material at <http://link.aps.org/supplemental/10.1103/PhysRevA.107.022803> for the tabulated inelastic squared form factors, generalized oscillator strengths, and differential cross sections of the vibronic states of deuterium molecule.
- [40] R. J. Buenker and R. A. Phillips, *J. Mol. Struct: Theochem.* **123**, 291 (1985).
- [41] S. Krebs and R. J. Buenker, *J. Chem. Phys.* **103**, 5613 (1995).
- [42] R. J. Buenker, M. Honigmann, H. P. Liebermann, and M. Kimura, *J. Chem. Phys.* **113**, 1046 (2000).
- [43] W. Q. Xu, Z. R. Ma, Y. G. Peng, X. J. Du, Y. C. Xu, L. H. Wang, B. Li, H. R. Zhang, B. Y. Zhang, J. H. Zhu, S. X. Wang, Y. Wu, J. G. Wang, and L. F. Zhu, *Phys. Rev. A* **103**, 032808 (2021).
- [44] W. Q. Xu, Y. G. Peng, J. H. Zhu, X. J. Du, Y. C. Xu, L. H. Wang, B. Li, H. R. Zhang, B. Y. Zhang, Z. R. Ma, S. X. Wang, Y. Wu, J. G. Wang, and L. F. Zhu, *Phys. Rev. A* **105**, 032801 (2022).
- [45] Y. W. Liu, Y. G. Peng, T. Xiong, S. X. Wang, X. C. Huang, Y. Wu, and L. F. Zhu, *J. Chem. Phys.* **150**, 094302 (2019).
- [46] C. C. Marston and G. G. Balint-Kurti, *J. Chem. Phys.* **91**, 3751 (1989).
- [47] H. Abgrall, F. Launay, and E. Roueff, *J. Chem. Phys.* **87**, 2036 (1987).
- [48] L. Wolniewicz, T. Orlikowski, and G. Staszewska, *J. Mol. Spec.* **238**, 118 (2006).
- [49] F. J. de Heer, *Phys. Scr.* **23**, 170 (1981).
- [50] S. J. Buckman and A. V. Phelps, *J. Chem. Phys.* **82**, 4999 (1985).